

Hematologic Malignancies of the Liver: Spectrum of Disease¹

Anderanik Tomasian, MD
Kumar Sandrasegaran, MD
Khaled M. Elsayes, MD
Alampady Shanbhogue, MD
Akram Shaaban, MD
Christine O. Menias, MD²

Abbreviations: AIDS = acquired immunodeficiency syndrome, AML = acute myeloid leukemia, FDG = fluorodeoxyglucose, GVHD = graft-versus-host disease, HCC = hepatocellular carcinoma, HIV = human immunodeficiency virus, HLH = hemophagocytic lymphohistiocytosis, PHL = primary hepatic lymphoma, PTLD = posttransplant lymphoproliferative disorder

RadioGraphics 2015; 35:71–86

Published online 10.1148/rg.351130008

Content Codes: **CT** **GI** **MR** **OI**

¹From the Mallinckrodt Institute of Radiology, Washington University School of Medicine, 510 S Kingshighway Blvd, St Louis, MO 63110 (A.T., C.O.M.); Department of Radiology, Indiana University School of Medicine, Indianapolis, Ind (K.S.); Department of Radiology, University of Texas MD Anderson Cancer Center, Houston, Tex (K.M.E.); Department of Radiology, University of Texas Health Science Center at San Antonio, San Antonio, Tex (A. Shanbhogue); and Department of Radiology, University of Utah, Salt Lake City, Utah (A. Shaaban). Recipient of a Cum Laude award for an education exhibit at the 2012 RSNA Annual Meeting. Received June 28, 2013; revision requested September 11 and received January 28, 2014; accepted April 3. For this journal-based SA-CME activity, the author K.S. has provided disclosures (see p 000); all other authors, the editor, and the reviewers have disclosed no relevant relationships. **Address correspondence to** A.T. (e-mail: tomasiana@mir.wustl.edu).

²Current address: Department of Radiology, Mayo Clinic, Scottsdale, Ariz.



Scan this code for access to supplemental material on our website.

The incidence of hematologic malignancies and their extranodal manifestations is continuously increasing. Previously unsuspected hepatic involvement in hematologic malignancies such as Hodgkin disease and non-Hodgkin lymphoma, posttransplant lymphoproliferative disorder, myeloid sarcoma (chloroma), multiple myeloma, Castleman disease, and lymphohistiocytosis may be seen by radiologists. Although the imaging features of more common hepatic diseases such as hepatocellular carcinoma, metastases, and infection may overlap with those of hepatic hematologic malignancies, combining the imaging features with clinical manifestations and laboratory findings can facilitate correct diagnosis. Clinical features that suggest a hematologic neoplasm as the cause of liver lesions include a young patient (<40 years of age), no known history of cancer, abnormal bone marrow biopsy results, fever of unknown origin, and night sweats. Imaging features that suggest hematologic malignancy include hepatosplenomegaly or splenic lesions, vascular encasement by a tumor without occlusion or thrombosis, an infiltrating mass at the hepatic hilum with no biliary obstruction, and widespread adenopathy above and below the diaphragm. Familiarity with the imaging features of hepatic hematologic malignancies permits correct provisional diagnosis and may influence therapeutic management. For example, when biopsy is performed, core biopsy may be needed in addition to fine-needle aspiration so that the tissue architecture of the neoplasm can be discerned. The predominant treatment of hematologic malignancies is chemotherapy or radiation therapy rather than surgery. *Online supplemental material is available for this article.*

©RSNA, 2015 • radiographics.rsna.org

SA-CME LEARNING OBJECTIVES

After completing this journal-based SA-CME activity, participants will be able to:

- Discuss the spectrum of hepatic hematologic malignancies.
- Describe the imaging and clinical features of primary and secondary hematologic malignancies of the liver.
- Recognize the imaging features of hepatic hematologic malignancies that assist in provisional diagnosis.

See www.rsna.org/education/search/RG.

Introduction

Hematologic malignancies include a wide spectrum of lymphoproliferative and myeloproliferative disorders with nodal and extranodal manifestations. Hepatic involvement is a common extranodal manifestation of common and some rare hematologic malignancies (1–3). Although the imaging features of some hepatic hematologic malignancies are nonspecific, some types have characteristic imaging features. When these features are combined with specific clinical manifestations, the possibility of hematologic malignancy of the liver may be raised. This may change

TEACHING POINTS

- In patients with PHL, distant lymphadenopathy (including superficial and mediastinal adenopathy), splenomegaly or splenic lesions, and bone marrow disease or a leukemic blood profile should not be seen for at least 6 months after the onset of hepatic disease.
- In patients who present de novo with focal liver masses, features that suggest the diagnosis of lymphoma include no known history of primary malignancy, young age (<40 years), B symptoms, splenic lesions, splenomegaly, and widespread abdominal or mediastinal lymphadenopathy.
- The incidence of PTLD and the prognosis vary according to the organ transplanted, recipient age, and intensity of immunosuppression therapy. The risk for developing PTLD is greatest within 1 year of transplantation and declines over time thereafter.
- Myeloid sarcoma (granulocytic sarcoma or chloroma) is a rare extramedullary proliferation of immature myeloid cells. It is most commonly seen in patients with AML and occurs in 3%–5% of these patients.
- Radiologically detectable extraosseous manifestations occur in 10%–16% of patients with multiple myeloma. The lymph nodes, pleura, and liver are the most commonly involved organs.

the diagnostic management in some circumstances. For instance, core biopsy may be required rather than fine-needle aspiration to improve diagnostic accuracy and reproducibility among pathologists (4). In addition, therapeutic management may be altered because the primary treatment of hematologic malignancies may be chemotherapy and/or radiation therapy rather than surgery.

In this article, we review the imaging features of hepatic hematologic malignancies, including Hodgkin disease and non-Hodgkin lymphoma, posttransplant lymphoproliferative disorder (PTLD), myeloid sarcoma (chloroma), multiple myeloma, Castleman disease, and hemophagocytic lymphohistiocytosis (HLH). The characteristic clinical and imaging findings of these diseases are described, and differential diagnosis is discussed. (For a concise summary, see Table E1.)

Primary and Secondary Hepatic Lymphoma

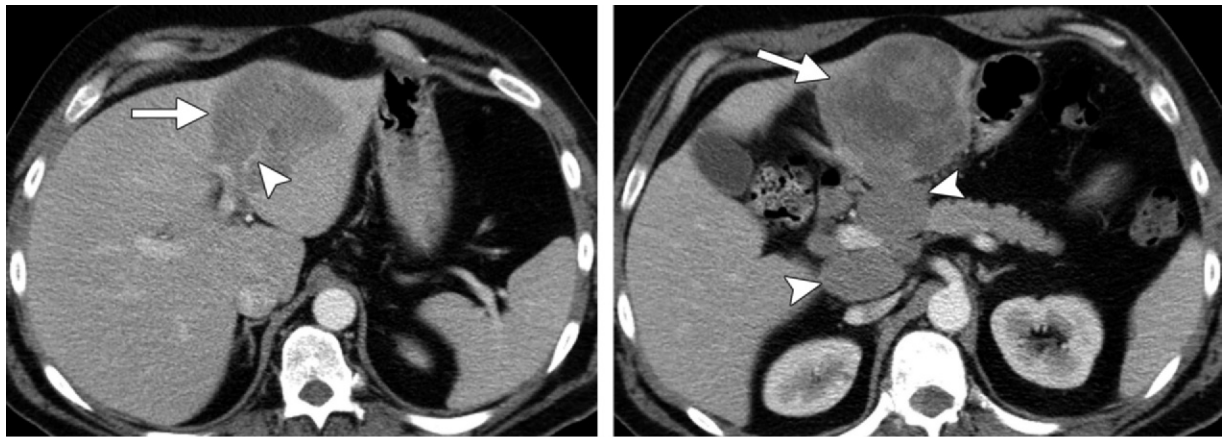
PHL is defined as lymphoma that is confined to the liver and perihepatic nodal sites at patient presentation, without distant involvement (5,6). PHL should be differentiated from lymphoma that secondarily affects the liver because the management and prognoses differ. Secondary liver involvement is seen in at least 50% of patients with non-Hodgkin lymphoma at autopsy. In contrast, PHL is rare and accounts for less than 1% of all non-Hodgkin lymphomas (7).

In patients with PHL, distant lymphadenopathy (including superficial and mediastinal ad-

enopathy), splenomegaly or splenic lesions, and bone marrow disease or a leukemic blood profile should not be seen for at least 6 months after the onset of hepatic disease (8). However, hepatic hilar adenopathy may be seen in PHL (Fig 1). More than 50% of patients with PHL present with right upper quadrant pain or jaundice. The B symptoms (systemic symptoms) of lymphoma, such as fever and weight loss, are found in about one-third of patients with PHL (6). PHL is commonly associated with viral hepatitis B and C and Epstein-Barr virus, but the pathophysiology of PHL is poorly understood. The incidence of PHL has increased in recent years, particularly in patients with human immunodeficiency virus (HIV) infection, predominantly because of immunosuppression. Most cases of PHL are of B-cell lineage (6,9).

Lymphomatous involvement of the liver may manifest at imaging as a discrete focal liver mass or masses, diffuse infiltrating disease, or an ill-defined mass in the porta hepatis (5,6,9–13). The most common imaging manifestation of PHL is a solitary discrete lesion, which is seen in about 60% of cases (Fig 1). Multiple lesions are seen in 35%–40% of patients (9), although one lesion is likely to be dominant (Fig 2). Diffuse infiltration is uncommon in PHL and indicates a poor prognosis (9). In contrast, multifocal lesions or diffuse infiltration is the most common pattern of secondary hepatic lymphoma (90%) (Fig 3). Numerous small discrete nodules (in a miliary pattern) are distributed throughout the liver in about 10% of cases of Hodgkin disease and secondary non-Hodgkin lymphoma of the liver (2) (Fig 4). Another point of distinction is that dominant liver masses are not typically seen in secondary lymphoma (2,12) but are characteristic of PHL (Fig 1). In addition, untreated nodules in secondary hepatic lymphoma are usually homogeneous, even when large (Figs 3, 5), while the dominant masses in PHL are typically heterogeneously enhancing (Figs 1, 2) (2,12). By definition, splenic lesions are not seen in patients with PHL but are seen in 30%–40% of patients with secondary non-Hodgkin lymphoma (Fig 3).

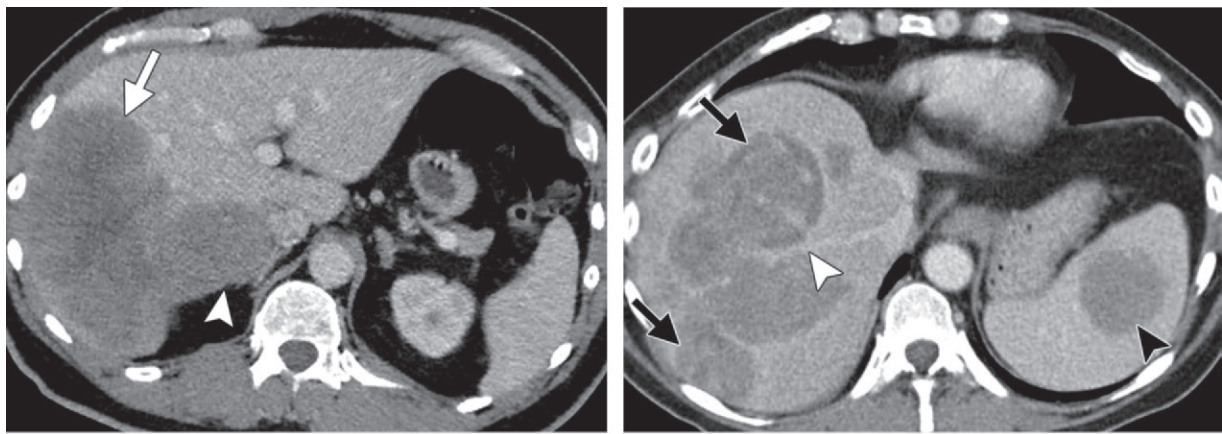
At US, the nodules usually are hypoechoic (Fig 6) or, rarely, anechoic and may resemble cysts. The absence of posterior acoustic enhancement indicates that the lesions are solid. Nodules may have a “target” appearance, with central hyperechoic and peripheral hypoechoic components (2,5). Increased peripheral vascularity in PHL nodules has been described at Doppler US and may mimic findings of hemangioma (11). The preliminary findings in a study of contrast-enhanced US suggest that PHL demonstrates mild



a.

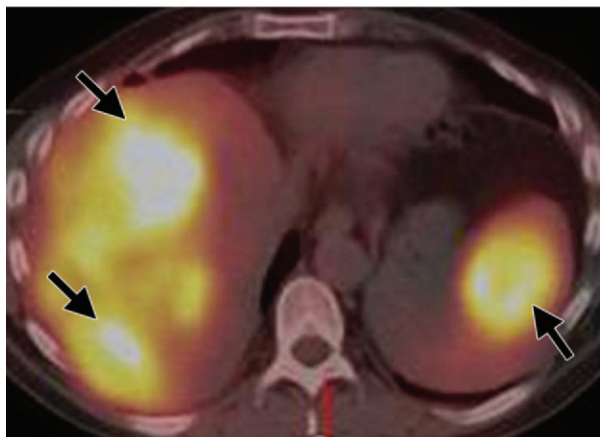
b.

Figure 1. PHL in a 51-year-old man with night sweats. Axial CT images show a solitary mass in the left lobe of the liver (arrow), with a patent vessel (arrowhead in a) seen coursing through the mass. The spleen is uninvolved. Periportal nodes are seen (arrowheads in b), but there is no other abdominal adenopathy. Lymphoma was suspected and was proven at biopsy.



2.

3a.



3b.

Figures 2, 3. (2) PHL in a 57-year-old man with fever and night sweats. Axial CT image shows two contiguous lesions (arrow and arrowhead) in the liver, with one lesion being dominant (arrow). Biopsy demonstrated lymphoma. No evidence of lymphoma outside the liver was seen at bone marrow biopsy or PET. (3) Secondary hepatic large B-cell non-Hodgkin lymphoma in an 83-year-old woman who presented for disease restaging. (a) Axial contrast-enhanced CT image shows multiple discrete homogeneously hypoenhancing hepatic masses (arrows) and a splenic mass (black arrowhead). The right hepatic vein (white arrowhead) is seen coursing through the mass without occlusion or constriction. (b) Axial fluorodeoxyglucose (FDG) PET/CT image shows avidly hypermetabolic lesions (arrows).

inhomogeneous hyperenhancement in the arterial phase and contrast agent washout in the portal and late phases (14).

At CT, lymphomatous nodules commonly have soft-tissue attenuation but enhance to a lesser degree than the liver parenchyma on arterial, portal venous, and delayed phase images (Figs 1–5). The

lesions may demonstrate hemorrhage, necrosis, or a rim-enhancement pattern (2,5,13). Calcification is rare in the absence of treatment. A multiphase CT study is not indicated for diagnosis of hepatic lymphoma because the lesions typically are hypovascular in all phases.

At MR imaging, the nodules tend to be hypo- or isointense on T1-weighted images and moderately hyperintense on T2-weighted images (Fig 7), with an enhancement pattern similar to that seen at CT. At T2-weighted MR imaging, a “target” appearance, with a hyperintense poorly enhancing

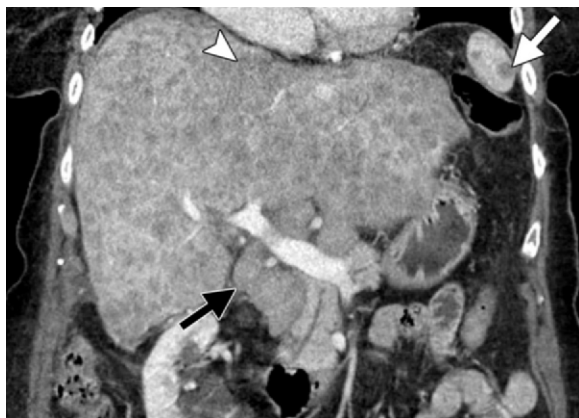


Figure 4. Miliary pattern in an 82-year-old man with secondary large B-cell hepatic lymphoma who presented with abdominal fullness. Coronal CT image shows multiple solid hypoenhancing masses (arrowhead) in a miliary pattern throughout the liver. Moderate periportal adenopathy (black arrow) and splenic lesions (white arrow) are also seen.

center and peripheral enhancement, has been described in about 15% of lesions (Fig 8). Diffusion-weighted MR imaging is an important component of the imaging protocol for characterization of suspected lymphomatous lesions. The highly cellular nature of lymphoma typically results in restricted diffusion. Diffusion-weighted imaging may allow earlier identification of disease in some cases when compared with traditional MR imaging sequences (Fig 7). Diffusion-weighted imaging has the benefit of not requiring intravenous contrast material. Whole-body diffusion-weighted imaging has been suggested to be as sensitive as FDG PET/CT (15–17) for lymphoma staging. FDG PET/CT typically demonstrates avid hypermetabolism (Fig 3) in both primary and secondary hepatic lymphoma (18–22). PET/CT is usually the imaging modality of choice for staging and for assessing treatment response.

The differential diagnosis includes hepatocellular carcinoma (HCC), which is substantially more common than PHL. Both HCC and PHL may occur in patients who have cirrhosis with viral hepatitis. Both neoplasms may be infiltrative, may show mild signal hyperintensity on T2-weighted MR images, and may demonstrate restricted diffusion (Fig 9). Imaging findings of lymphadenopathy below the level of the renal veins, poor lesion enhancement in all contrast-enhanced phases, and vascular encasement without thrombosis favor a diagnosis of lymphoma (2,23). Imaging findings of arterial phase enhancement, delayed contrast material washout with capsular enhancement, and vascular thrombosis suggest HCC. In general, hepatic lymphomas are avidly hypermetabolic at PET, while most HCCs are not (18,24).

In a patient with lymphoma who is undergoing chemotherapy, focal liver lesions may be due to

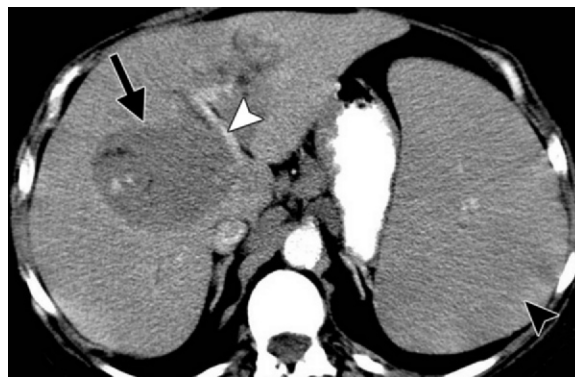


Figure 5. Differentiating primary from secondary hepatic lymphoma in a 77-year-old woman with known lymphoma who presented with splenomegaly at physical examination. Axial CT image shows hepatomegaly with discrete, predominantly homogeneous, hypoenhancing masses (arrow). An unaffected vessel (white arrowhead) is seen coursing through the mass, and splenomegaly is also seen (black arrowhead). The combination of hepatosplenomegaly and vessel encasement without occlusion suggests a hematologic disorder. Secondary lymphoma is associated with splenomegaly and homogeneous masses.

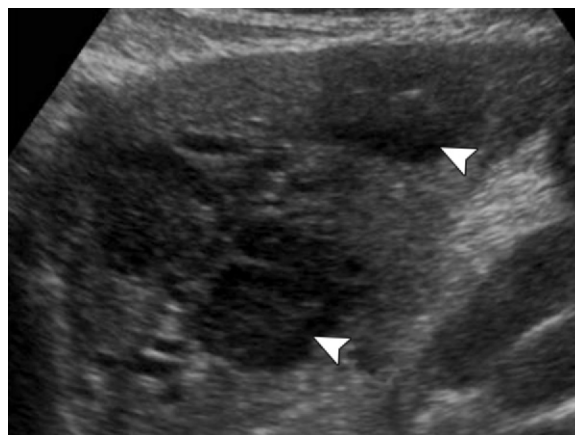


Figure 6. Primary large B-cell hepatic lymphoma in an 83-year-old woman with elevated results on liver function tests. US image shows multiple solid heterogeneously hypoechoic masses (arrowheads). This imaging finding cannot be differentiated from metastatic cancer.

reasons other than lymphomatous involvement, such as infection or, rarely, drug toxicity. Opportunistic infections such as fungal microabscesses and septic emboli are the two most common differential diagnoses for secondary hepatic lymphoma (Fig 10) (2). A diagnosis of fungal microabscess is favored if there is a history of immunosuppression, fever, or an abnormal white blood cell count. Although CT may depict perilesional hyperemia in fungal microabscesses, the imaging features may overlap with those of PHL, and tissue sampling may be warranted for definitive diagnosis. Metastases from cancer may also manifest as multiple FDG-avid hypoenhancing hepatic lesions but would be a less likely consideration in

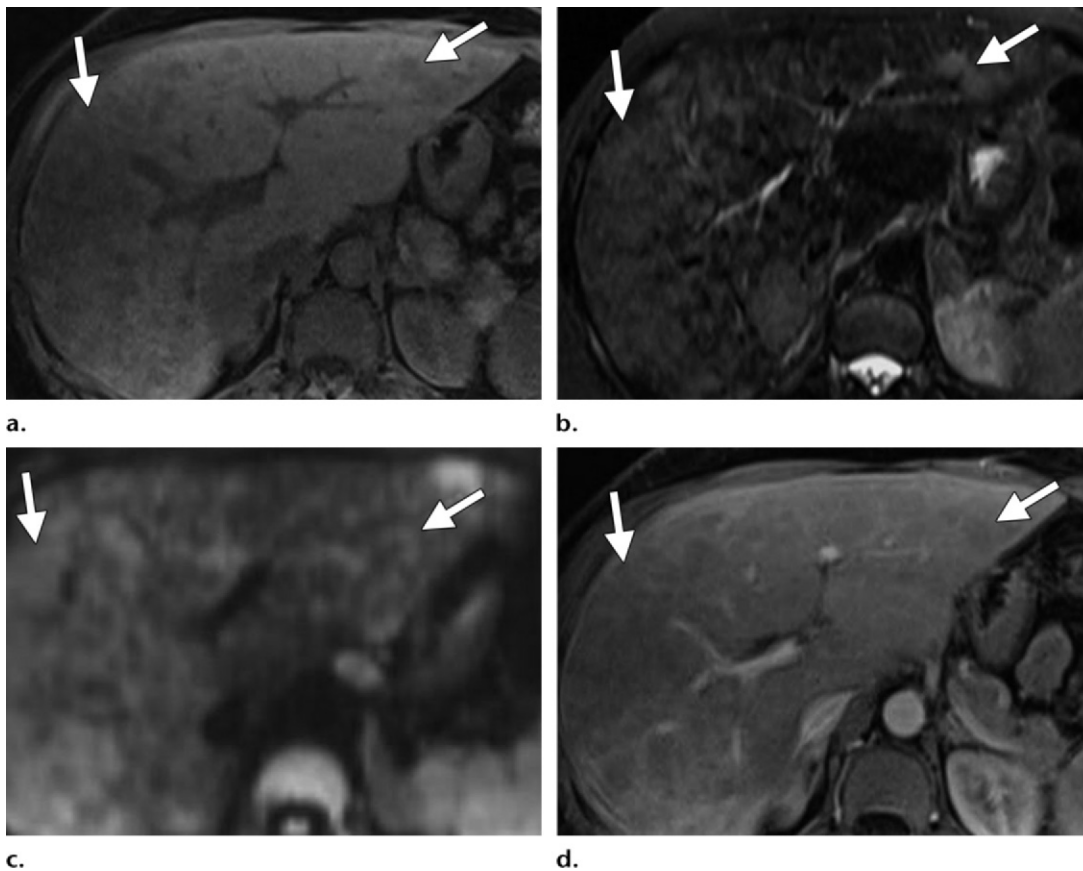


Figure 7. Hepatic lymphoma in a 56-year-old woman in whom vague hepatic lesions were seen on initial CT images. (a, b) Axial T1-weighted (a) and T2-weighted (b) MR images show numerous nodules (arrows), some confluent, which are hypointense on the T1-weighted image and hyperintense on the T2-weighted image. (c) Diffusion-weighted MR image ($b = 500 \text{ sec/mm}^2$) shows the lesions (arrows) as hyperintense relative to the liver, a finding suggestive of restricted diffusion. (d) Axial gadolinium-enhanced MR image shows mildly hypoenhancing lesions (arrows) that are not as well depicted as in b and c.

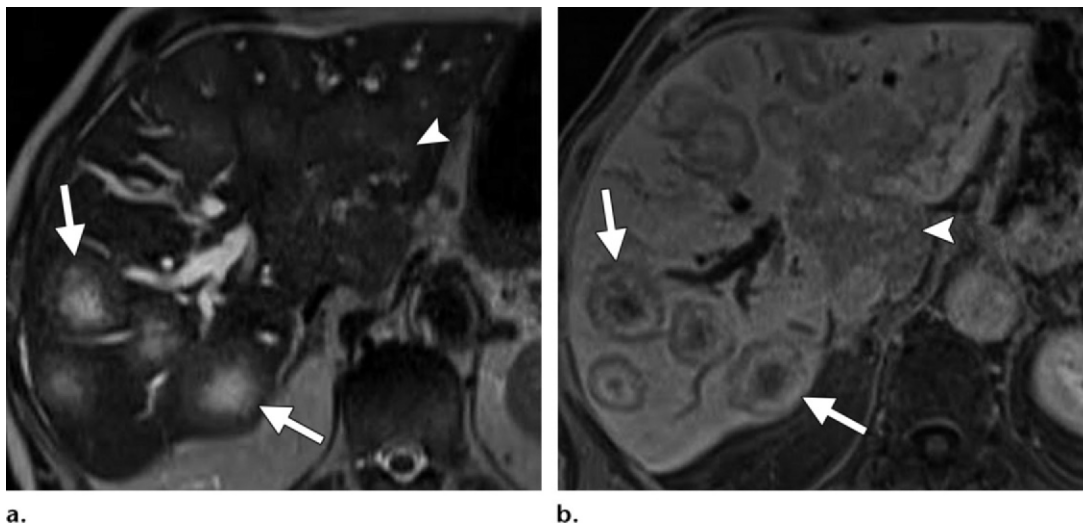


Figure 8. “Target” appearance of lesions in an 80-year-old man with large B-cell secondary hepatic lymphoma. (a) Axial T2-weighted MR image shows multiple hepatic lesions (arrows) with a targetlike appearance, with a hyperintense center and a hypointense periphery. A more infiltrative mass (arrowhead) in the porta hepatis extends into the left lobe and obstructs the bile duct. (b) Axial gadolinium-enhanced MR image shows the targetlike lesions (arrows) with poorly enhancing centers. The ill-defined infiltrating mass (arrowhead) is seen in the porta hepatis.

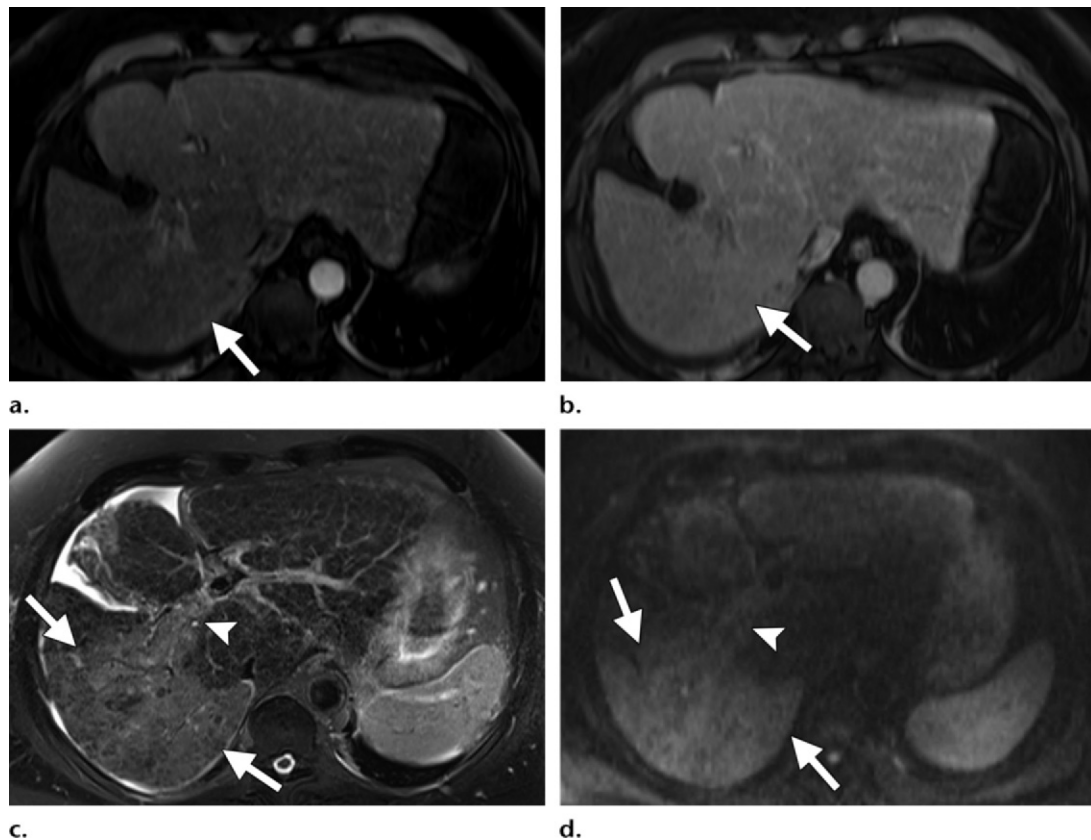
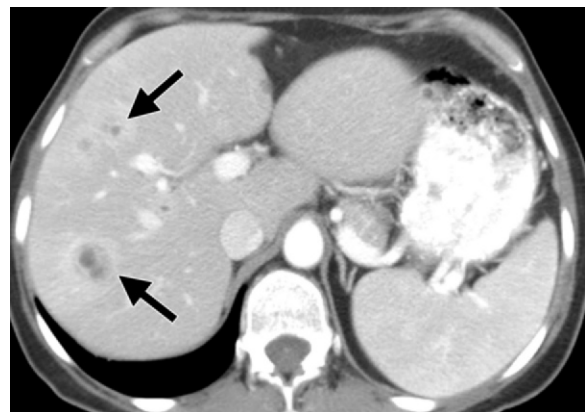


Figure 9. Infiltrative HCC in a 67-year-old man with cirrhosis and elevated α -fetoprotein levels. (a, b) Axial gadolinium-enhanced arterial phase (a) and venous phase (b) MR images show no discernible abnormality in the right lobe of the liver (arrow). (c) Axial T2-weighted MR image shows definite signal hyperintensity in the right posterior lobe (arrows), with extension of high signal intensity into the right portal vein (arrowhead). (d) Diffusion-weighted MR image ($b = 500 \text{ sec/mm}^2$) shows signal hyperintensity in the right lobe (arrows) and right portal vein (arrowhead), findings that suggest focal restricted diffusion. The findings in c and d are suspicious for infiltrating HCC. Biopsy demonstrated poorly differentiated HCC.

Figure 10. Fungal microabscesses in a 52-year-old woman with AML who presented with fever. Axial CT image shows small, ill-defined, low-attenuating hepatic masses (arrows) with surrounding hyperemia. Guided liver biopsy demonstrated fungal microabscesses.



cases of known lymphoma. In patients who present de novo with focal liver masses, features that suggest the diagnosis of lymphoma include no known history of primary malignancy, young age (<40 years), B symptoms, splenic lesions, splenomegaly, and widespread abdominal or mediastinal lymphadenopathy.

Hepatic lymphoma is typically treated with chemotherapy, with the treatment regimen dictated by the histologic subtype. Therefore, suggesting the diagnosis of hepatic lymphoma versus HCC, metastasis, or infection contributes to appropriate management because surgery or liver-directed therapy (for HCC and metastasis) and antibiotic administration and drainage (for infection) may be obviated.

Posttransplant Lymphoproliferative Disorder

The development of PTLD after solid organ transplantation remains a challenging diagnostic and therapeutic problem. Epstein-Barr virus infection has been linked to 85% of PTLD cases (1,25). Epstein-Barr virus is thought to induce prolonged activation in B lymphocytes (in 85% of cases), which may lead to an irreversible

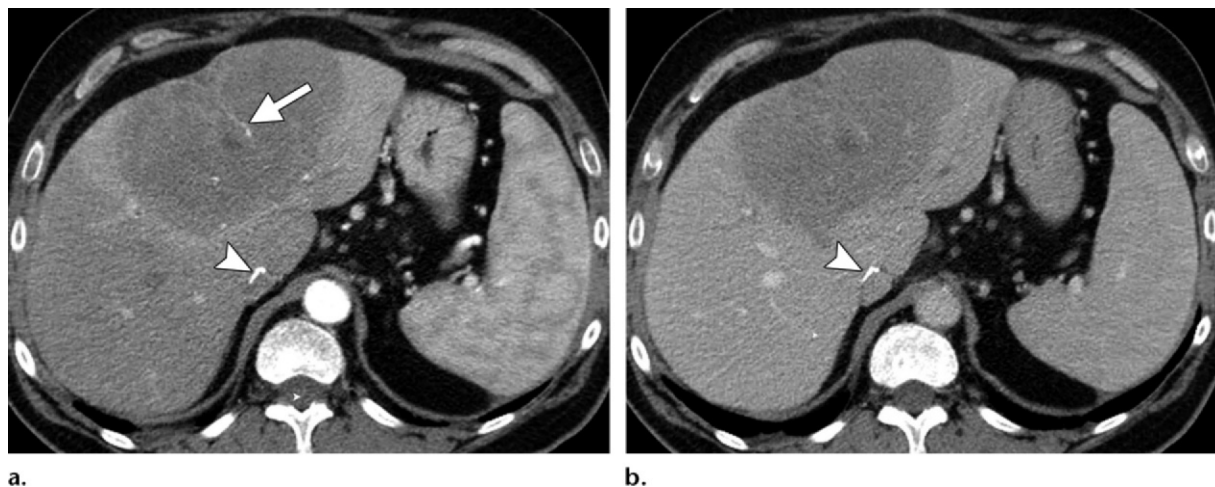


Figure 11. PTLD in a 61-year-old man who presented with abdominal fullness 9 months after orthotopic liver transplant. Axial arterial phase (a) and venous phase (b) CT images show a large, well-defined, hypoenhancing mass in the left lobe, with a preserved small artery (arrow in a). Surgical clips from inferior vena cava anastomosis are seen (arrowhead). Biopsy demonstrated PTLD.

transforming genetic event (1). T-cell, natural killer cell, and plasma cell activation have also been described in PTLD, although they are rare. The American Society for Transplantation has reported that the term may be applied to post-transplant infectious mononucleosis and plasma cell hyperplasia (reactive hyperplasia) in addition to neoplastic disease. When the term is not qualified, it usually refers to monomorphic neoplastic disease (26). The World Health Organization classification system describes four major histopathologic subtypes of PTLD: early hyperplastic lesions, polymorphic lesions, monomorphic lesions, and classic Hodgkin-type lymphomas (27,28). However, a recent expert panel has made additional changes to the PTLD classification because the current classification system correlates poorly with treatment options and prognosis (29). The latest classification system takes into account histology, Epstein-Barr virus clonality, the Epstein-Barr virus status of the recipient, and tumor localization. The following section discusses malignant monomorphic PTLD.

The incidence of PTLD and the prognosis vary according to the organ transplanted, recipient age, and intensity of immunosuppression therapy. The risk for developing PTLD is greatest within 1 year of transplantation and declines over time thereafter (30). The frequency of PTLD is substantially higher in pediatric recipients, who are more likely to be Epstein-Barr virus seronegative than are adults and thus are more prone to transplant-induced Epstein-Barr virus infection (31). The prevalence of PTLD is reported to be 1%–10% after solid organ transplant (1,25,32), and PTLD occurs after liver transplant in 2%–7% of cases. The prevalence of PTLD is reported as 5%–20% after small bowel and lung transplants

(31). Unlike lymphoma in the general population, PTLD has a high propensity for extranodal involvement (80%). The liver is the most commonly involved abdominal organ (50%), followed by the small bowel (25%) and kidneys (17%) (33).

At CT and MR imaging, three patterns of PTLD are seen. The most common manifestation of PTLD in the liver is one or more poorly enhancing masses (Figs 11, 12) (33,34). Occasionally, an ill-defined, heterogeneous, infiltrating mass is seen (31,33–36). When there is an infiltrative tumor, T2-weighted or diffusion-weighted MR images may better depict disease compared with gadolinium-enhanced MR images (Fig 11). A third pattern, characterized by a mass in the porta hepatis with biliary tree involvement and periportal lymphadenopathy, may be a characteristic feature of PTLD in liver transplant recipients (33) (Figs 13, 14). The portal vessels may be encased and occasionally are constricted. Vascular thrombosis or occlusion does occur but is substantially less common in PTLD than in other hepatic malignancies such as HCC or cholangiocarcinoma. In our review of patients with hepatic PTLD for this article, we found that three of 19 patients had portal vein constriction or focal thrombi. Other imaging manifestations of PTLD include splenomegaly or splenic lesions, gallbladder or bowel wall thickening, biliary obstruction, and adenopathy. PET is considered to be more accurate than CT or MR imaging for disease staging and assessing response to therapy, with active lesions being extremely hypermetabolic at PET (37,38).

It may be difficult to differentiate the discrete hepatic lesions of PTLD from findings of opportunistic infection in posttransplant patients. Serology, cultures, and sometimes liver biopsy are required for clarification. PTLD may occur

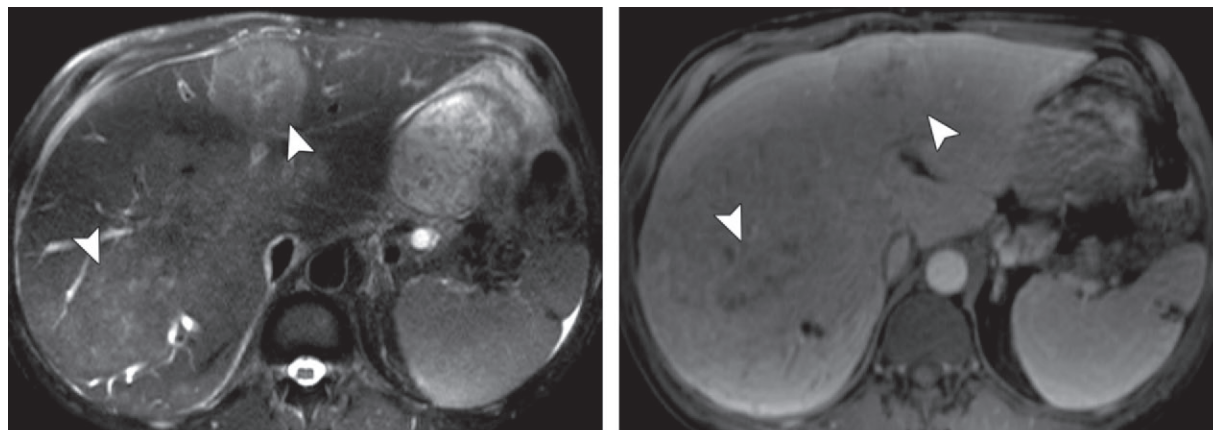
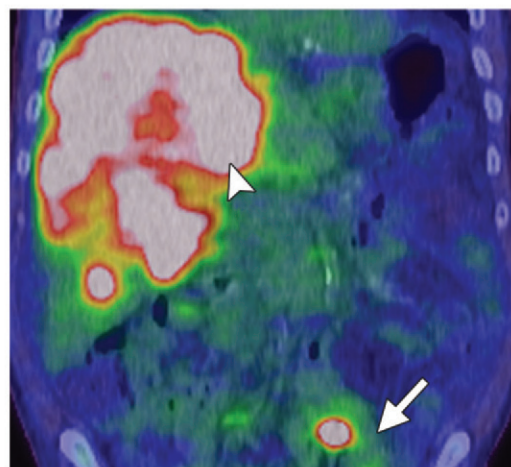


Figure 12. PTLD in a 56-year-old man with elevated liver function test results 6 months after kidney transplant. **(a)** Axial T2-weighted MR image shows multiple poorly defined, mildly hyperintense hepatic masses (arrowheads). **(b)** Axial contrast-enhanced venous phase MR image shows barely visible lesions (arrowheads) in both lobes. **(c)** Coronal fused FDG PET/CT image shows the lesions as avidly hypermetabolic (arrowhead). Note the transplanted kidney (arrow).



in patients who underwent orthotopic liver transplant for cirrhosis with HCC. It usually is possible to differentiate PTLD from recurrent HCC on the basis of imaging characteristics (Fig 15). The most common pattern of HCC recurrence after liver transplant is multiorgan involvement (39). The organs most commonly affected by recurrent HCC after transplant are the liver (62%), lungs (56%), and bones (18%) (40).

PTLD is typically treated with a reduction in immunosuppression therapy, which allows restoration of Epstein-Barr virus-specific cytotoxic T lymphocytes (32). Refractory cases may be treated with antiviral therapy and/or chemoradiation (28,32).

Myeloid Sarcoma

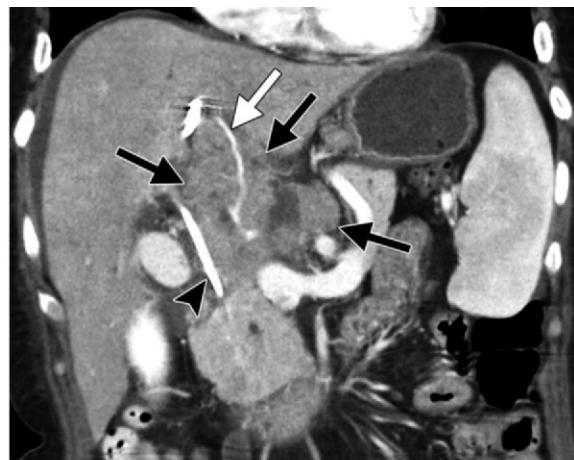
Myeloid sarcoma (granulocytic sarcoma or chloroma) is a rare extramedullary proliferation of immature myeloid cells. It is most commonly seen in patients with AML (41–44) and occurs in 3%–5% of these patients (43). The incidence of myeloid sarcoma is increasing as patients with AML undergo intensive chemotherapy and bone marrow transplant. Myeloid sarcoma is associated with other myeloproliferative conditions, such as chronic myeloid leukemia and myelodysplastic syndrome, and is uncommonly associated with essential thrombocythemia and polycythemia vera (44). Myeloid sarcoma may manifest during remission or relapse of the underlying hematologic disease and has been reported to occur during remission of a hematologic malignancy in up to 20% of cases (44). It rarely may predate the onset of AML (41,44). At histopathologic analysis, myeloid sarcoma consists of my-

eloid blasts or precursor cells, with or without maturation. At immunohistochemical analysis, myeloid sarcoma stains positive for myeloperoxidase, which results in green staining of the lesions (hence the term *chloroma*). Cytogenetic abnormalities such as t(8;21) chromosomal translocation, blast differentiation, cell-surface markers, and lack of Auer rods have been associated with a higher incidence of extramedullary leukemia (45). A diagnosis of myeloid sarcoma indicates a poor outcome, irrespective of the clinical manifestations. Given the influence of the diagnosis of myeloid sarcoma on the prognosis, radiologists should recognize the distribution and imaging features of myeloid sarcoma.

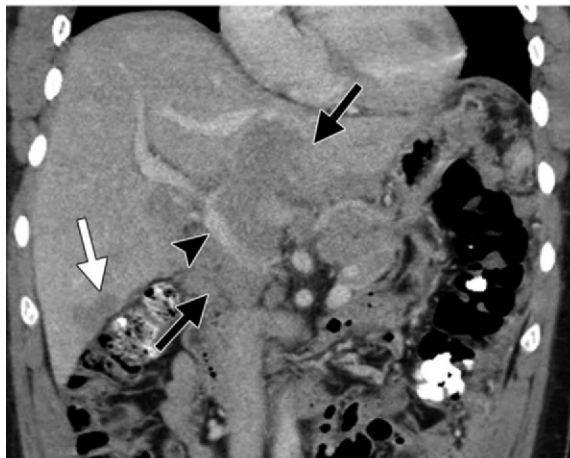
The most common sites of myeloid sarcoma involvement are the bones, lymph nodes, soft tissues, skin, and breasts. Less common sites are the genitourinary tract, gastrointestinal system, head and neck, and thorax (41,44). The imaging features of hepatic myeloid sarcoma are nonspecific and are similar to those of hepatic lymphoma. However, despite nonspecific imaging findings, the diagnosis of myeloid sarcoma can be made in the clinical context of known AML. Discrete masses



13a.



13b.

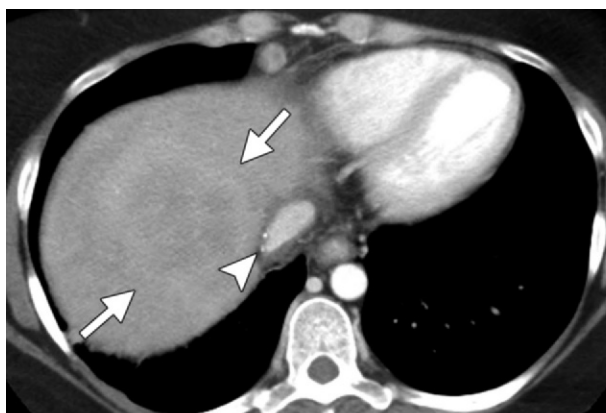


14a.

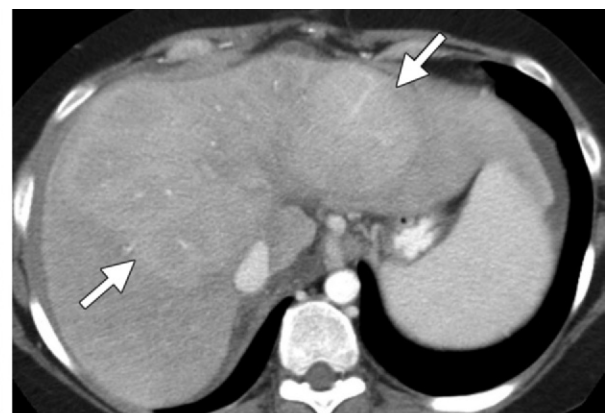


14b.

Figures 13, 14. (13) Periportal infiltrative pattern of PTLD in a 69-year-old woman with previous liver transplant who presented with abdominal pain. (a) Axial CT image shows a poorly defined mass (arrow) in the periportal region. The mass is causing biliary obstruction, and a biliary stent is seen (black arrowhead). Focal nonocclusive portal vein thrombosis is also seen (white arrowhead). (b) Coronal reformatted CT image shows the mass (black arrows) and biliary stent (arrowhead). The hepatic artery (white arrow) runs through the mass without occlusion. (14) PTLD manifesting as a periportal mass in a 35-year-old man with a history of liver transplant who presented with abdominal tenderness. (a) Coronal reformatted CT image shows a large periportal mass (black arrows) enveloping but not occluding the main portal vein (arrowhead). The tumor also involves the liver (white arrow). (b) Coronal reformatted CT image obtained after medical therapy shows complete resolution of the mass.



a.



b.

Figure 15. Differentiation of PTLD from HCC in a 54-year-old woman who underwent orthotopic liver transplant for cirrhosis with HCC and presented for routine HCC screening. Axial CT images show a large mildly hyperenhancing mass (arrows), with patent vessels seen coursing through the mass in b. Surgical clips are seen in the inferior vena cava (arrowhead in a). The findings are suspicious for PTLD rather than recurrent HCC. Biopsy demonstrated PTLD.

of myeloid sarcoma typically are more heterogeneously enhancing and less well circumscribed than those of hepatic lymphoma (Fig 16). The diffuse hepatic sinusoidal infiltration of leukemic cells may result in intra- or extrahepatic biliary duct obstruction (46). FDG PET/CT is useful in early detection when the disease is clinically occult. It also allows disease staging and treatment monitoring (41,42). Myeloid sarcoma is treated with chemotherapy or localized radiation therapy (47,48).

The liver may be affected by other diseases in patients who have received a stem cell allograft for hematologic malignancies. These diseases include sinusoidal obstruction syndrome (veno-occlusive disease), acute graft-versus-host disease (GVHD), nodular regenerative hyperplasia, drug toxicity, PTLN, extramedullary hematopoiesis, atypical infections, and myeloid sarcoma. In particular, focal lesions of myeloid sarcoma should be differentiated from the more common acute GVHD (Fig 17) and fungal infections that occur in these patients with neutropenia (Fig 10). A detailed discussion of each of these entities is beyond the scope of this article. Table E2 summarizes the major features of some of these disorders (31,34,49–51).

Multiple Myeloma and Solitary Plasmacytoma

Multiple myeloma is characterized by the uncontrolled clonal proliferation of plasma cells originating from the bone marrow and usually is associated with the production of monoclonal paraprotein. Myeloma accounts for about 10% of malignant hematologic neoplasms (52,53). Extraosseous myeloma was once thought to be rare, but autopsy series have shown extraosseous disease in up to 64% of patients with myeloma (54). Radiologically detectable extraosseous manifestations occur in 10%–16% of patients with multiple myeloma (55). The lymph nodes, pleura, and liver are the most commonly involved organs. Extraosseous disease is more common in younger patients with myeloma and in those with more aggressive subtypes of myeloma (nonsecretory myeloma and immunoglobulin D myeloma) (55). Extraosseous involvement is associated with a poorer prognosis.

In autopsy studies, the reported prevalence of hepatic involvement in myeloma is about 30% (54). Extraosseous disease is seen in the majority (64%) of patients with myeloma at autopsy, with hepatic involvement seen in 28%–30% of patients (54). However, longitudinal cohort studies that used contrast-enhanced cross-sectional imaging have reported extraosseous myeloma in only 13% of cases (55). This discrepancy suggests that contrast-enhanced cross-sectional imaging

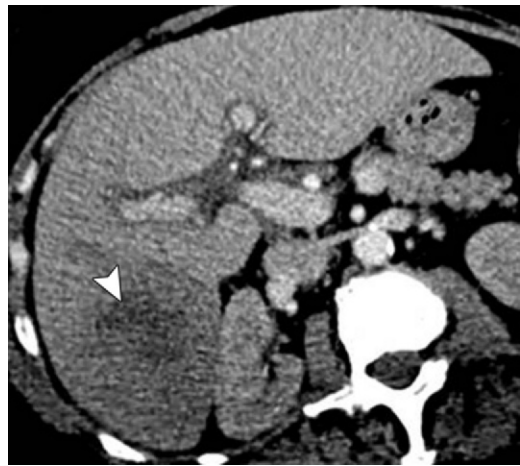


Figure 16. Myeloid sarcoma in a 64-year-old man with myelofibrosis who presented for imaging at an outside institution. Axial nonenhanced CT image shows a poorly defined hypoattenuating hepatic mass (arrowhead). The finding is nonspecific, but myeloid sarcoma is a leading consideration for a large mass in a patient with a myelogenous hematologic disorder. Biopsy demonstrated myeloid sarcoma.

is not performed in most patients with end-stage myeloma (perhaps because of renal dysfunction) or that CT and MR imaging are relatively insensitive for detection of hepatic involvement by myeloma. Hepatic involvement may be unifocal, multifocal, or diffuse (53,54). Liver involvement may be asymptomatic or may manifest as hepatomegaly, jaundice, ascites, or fulminant liver failure. Liver dysfunction in a patient with multiple myeloma can result from plasma cell infiltration or amyloidosis (56), and pathologic confirmation is often required.

Focal hepatic lesions are often hypoechoic at US. A targetlike appearance (an isoechoic nodule with a hypoechoic rim), mixed echogenicity, and, rarely, hyperechoic nodules have been described at US (53,57,58). At CT, the most common finding is hepatomegaly. Focal hepatic lesions are typically hypoattenuating, without calcification or substantial contrast enhancement (Fig 18) (52,53,57). Nonenhancing hyperattenuating lesions as well as hypervascular hepatic lesions have been rarely reported (53). Biliary obstruction may occur.

Myelomatous lesions are usually hyperintense on T1-weighted and T2-weighted MR images (52,53,57,59,60). Hyperintensity on T1-weighted images is presumably due to the high concentration of light chain protein in the lesions (60). There often is minimal enhancement on gadolinium-enhanced images. As with other infiltrative lesions, myelomatous lesions may be better depicted on T2-weighted images than on gadolinium-enhanced images (Fig 19). At FDG PET/CT, hepatic multiple myeloma demonstrates

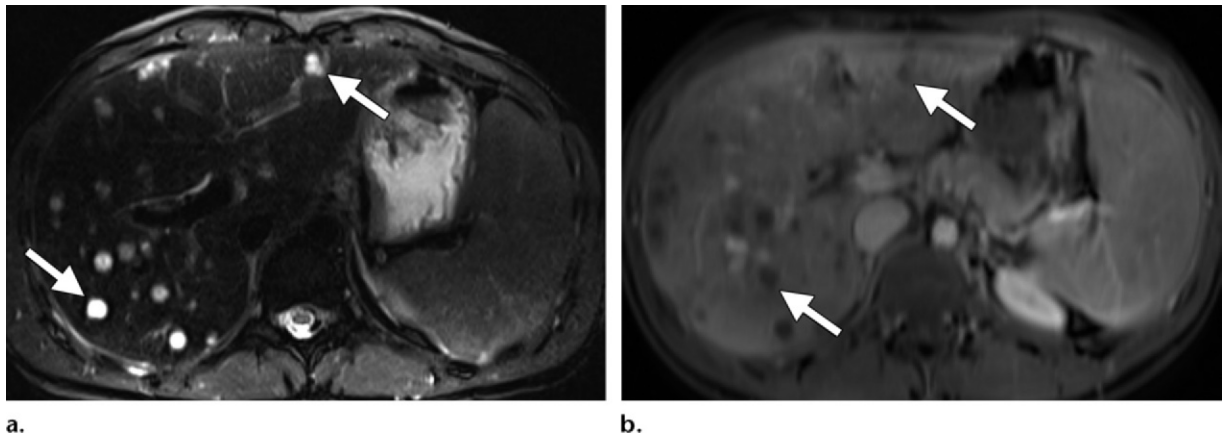


Figure 17. Acute GVHD in a 21-year-old man with fever and an elevated white blood cell count 6 weeks after hemopoietic stem cell transplant. **(a)** Axial T2-weighted MR image shows multiple hyperintense hepatic nodules (arrows) with hypointense rims. The spleen is not affected. No adenopathy was seen. **(b)** Axial gadolinium-enhanced T1-weighted MR image shows poor central enhancement of the nodules (arrows), with mild peripheral enhancement. A fungal infection was suspected, but biopsy demonstrated acute GVHD.



Figure 18. Extrasosseous myeloma in a 37-year-old woman with bone lesions. Axial CT image obtained to locate a possible primary malignancy shows multiple solid lesions in the liver (arrowheads) and spleen (arrow). The lesions are mildly hypoenhancing and do not show calcification. Biopsy of one of the liver lesions demonstrated myeloma.

moderate to intense FDG uptake (53). The imaging findings are nonspecific and may easily be confused with those of metastatic liver lesions, especially in the absence of a clinical history of myeloma. The final diagnosis is often confirmed with tissue sampling.

Solitary plasmacytoma is an extramedullary malignant proliferation of plasma cells in the absence of systemic myeloma. Systemic myeloma is excluded by a negative skeletal survey; the absence of clonal proliferation of plasma cells at bone marrow biopsy; and the absence of hypercalcemia, anemia, and renal involvement of the myeloma. Hepatic plasmacytoma is rare, and patients with this tumor usually progress to full-blown myeloma. The US, CT, and MR imaging appearances are variable and nonspecific. Lesions are hypermetabolic at PET, a finding that can be used to monitor response to therapy. If surgical resection of the tumor is not possible, radiation therapy is usually performed. The prognosis for patients with solitary plasmacytoma of the liver is better than for those with systemic myeloma.

Multiple myeloma is often treated with systemic chemotherapy (41,42). The standard melphalan-based combined chemotherapy is still used. However, therapy for myeloma is rapidly evolving. Treatment is now becoming individually tailored on the basis of many factors, including tumor burden, chromosomal translocations, genomic instability, and patient age. Newer drug therapies include immunomodulators such as bortezomib, thalidomide, carfilzomib, and pomalidomide (61–63). Stem cell transplant is also indicated in selected patients (64).

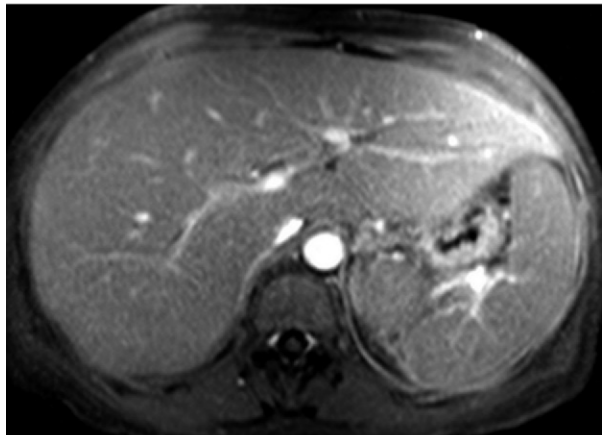
Castleman Disease

Castleman disease (angiofollicular lymph node hyperplasia or giant lymph node hyperplasia) is a nonclonal lymphoproliferative disorder and is one of the more common causes of lymphadenopathy, as a result of lymph node hyperplasia. This disease is associated with the unregulated overproduction of interleukin-6 (65,66). Castleman disease is most commonly found in the chest (70%), followed by the neck (15%), abdomen, and pelvis (15%) (66). The lymph nodes are the most commonly affected organ system. Extralymphatic sites of involvement include the lungs, larynx, parotid glands, pancreas, meninges, and muscles (65). Liver involvement is uncommon

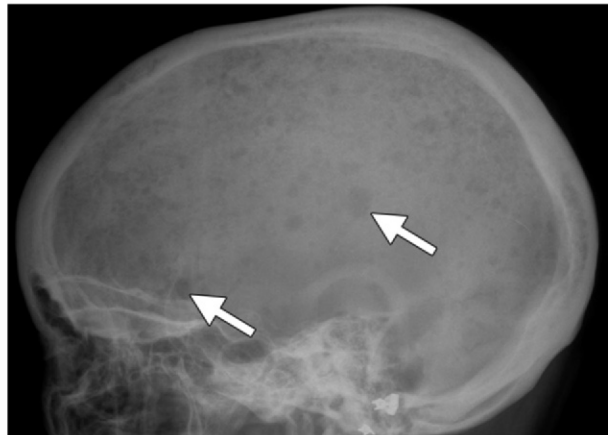
Figure 19. Extrasosseous myeloma in a 61-year-old woman with known myeloma and abnormal liver function test results. (a) Axial T2-weighted MR image shows minimally hyperintense hepatic lesions (arrowheads). (b) Axial gadolinium-enhanced MR image does not depict the hepatic lesions. (c) Lateral skull radiograph shows numerous lytic lesions (arrows), a finding consistent with the diagnosis of extrasosseous myeloma.



a.



b.



c.

(65–67). Castleman disease is classified as hyaline vascular or plasma cell type (68). An uncommon human herpesvirus 8–associated Castleman disease is also recognized.

Hyaline vascular Castleman disease accounts for 90% of cases. It typically occurs in young adults, usually affects a single site, and tends to have a benign course (65,66). Plasma cell–type disease represents less than 10% of cases and often is multicentric. The uncommon human herpesvirus 8–associated Castleman disease is seen in patients with acquired immunodeficiency syndrome (AIDS) and is associated with a poor prognosis (65,66).

Three patterns of involvement have been described: (a) a solitary noninvasive mass (50% of cases), (b) a dominant infiltrative mass with associated lymphadenopathy (40% of cases), and (c) matted lymphadenopathy without a dominant mass (10% of cases) (65,69). Dominant hepatic masses are seen with hyaline vascular Castleman disease. The lesions typically demonstrate homogeneous avid attenuation at CT (Fig 20). In contrast, an infiltrative periportal mass is associated with the plasma cell variant of Castleman disease. The plasma cell type typically

demonstrates less intense contrast enhancement compared with the hyaline vascular form (65), which makes differentiation from other causes of lymphadenopathy more challenging. Central areas of hypoattenuation due to fibrosis or necrosis may be seen in lesions larger than 5 cm. Nonspecific calcifications may be seen occasionally. Increased FDG uptake at PET/CT is typical. At MR imaging, lesions demonstrate heterogeneous signal intensity on T1- and T2-weighted images, with internal flow voids that represent the feeding vessels and intense contrast enhancement. The imaging features of human herpesvirus 8–associated Castleman disease are indistinguishable from those of the plasma cell variant (65).

Human herpesvirus 8 is the viral agent of Kaposi sarcoma. Multicentric Castleman disease due to this virus is often seen in patients with HIV infection. In patients with AIDS, the differential diagnosis for adenopathy and focal liver lesions includes Castleman disease, Kaposi sarcoma, *Mycobacterium tuberculosis* infection, *Mycobacterium avium-intracellulare* complex, AIDS-related lymphoma, bacillary angiomatosis, and fungal infections such as histoplasmosis



Figure 20. Castleman disease in a 47-year-old woman. Axial contrast-enhanced CT image shows a homogeneously hyperattenuating periportal nodal mass (arrowhead) and retroperitoneal nodes. Biopsy of a mediastinal lymph node (not shown) demonstrated Castleman disease.

(70,71). Adenopathy in mycobacterial infections and AIDS-related lymphoma tends to be hypoenhancing (70). Lymphadenopathy is not a major manifestation of opportunistic infections such as cytomegalovirus or of protozoa such as *Cryptosporidium* species (70).

Unicentric hyaline vascular Castleman disease is often curable with surgery. For patients who are not surgical candidates, localized radiation therapy may be curative (72,73). Chemotherapy is used in patients with inadequate surgical excision and those with multicentric disease. Several different regimens are used, including conventional chemotherapy agents such as steroids and cyclophosphamide. Many patients with multicentric Castleman disease, particularly those with HIV, are immunosuppressed and do not tolerate standard chemotherapy. Antiviral therapy for human herpesvirus 8 or highly active antiretroviral therapy is helpful in selected cases (72,73). Rituximab is a monoclonal anti-CD20 antibody. It is often used as a first-line therapy in patients with multicentric Castleman disease (72,74). Immunomodulators such as interferon and thalidomide have been tried. The newest agents are monoclonal antibodies that target interleukin-6 or its receptors. Siltuximab (anti-interleukin-6 antibody) and tocilizumab (anti-human interleukin-6 receptor antibody) have been used successfully in early trials (72).

Hemophagocytic Lymphohistiocytosis

HLH, or hemophagocytic syndrome, is a multi-system disorder characterized by cytokine dysfunction that results in uncontrolled proliferation of activated cytotoxic T cells, antigen-presenting cells, macrophages, and histiocytes (75–79). The diagnostic criteria include fever, splenomegaly, cytopenia that affects more than two cell lines, hypertriglyceridemia, hyperferritinemia (>500 $\mu\text{g/L}$), low fibrinogen level, and hemophagocytosis in the reticuloendothelial system (76). Early clinical signs associated with HLH include fever

(90% of cases), hepatosplenomegaly (90%), lymphadenopathy (42%), rashes, and neurologic abnormalities (47%) (75–79).

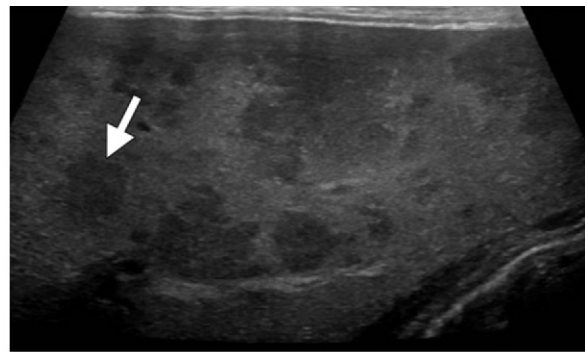
HLH manifests as either primary disease or secondary reactive disease. The primary form (familial or sporadic) occurs in young infants and results from genetic abnormalities that lead to defects in the immune system. The secondary form is usually seen in adults and occurs in response to infective agents, rheumatologic disorders, and malignancies. It is more commonly seen in immunocompromised individuals (76,77,79). This form is usually self-limiting but may require chemotherapy or immunomodulation.

At US, HLH lesions typically are solid and hypoechoic, with no discernible internal vascularity (Fig 21). At CT, solid hypoenhancing nodules are seen (Fig 21). The lesions are heterogeneously hypointense on T1-weighted MR images and hyperintense on T2-weighted images, with mild enhancement. Hepatosplenomegaly and diffuse lymphadenopathy are usually seen (Fig 21). Differentiation from metastatic cancer or lymphoma may not be possible without biopsy.

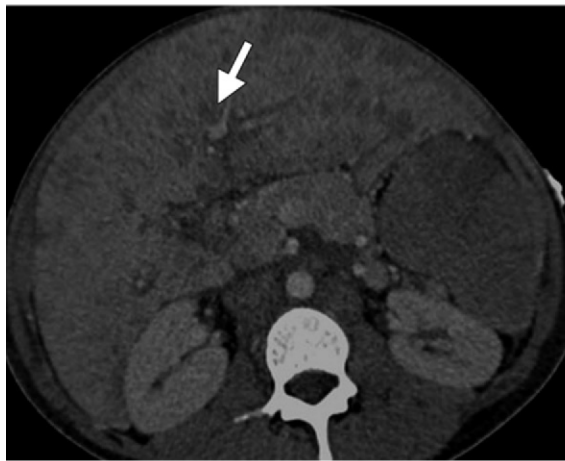
Conclusions

Hepatic hematologic malignancies include a wide spectrum of lymphoproliferative and myeloproliferative disorders. In many cases, knowledge of the clinical manifestations and imaging findings will raise concern for a hematologic disease involving the liver. Criteria that suggest hematologic disease include patient age younger than 40 years, B symptoms of lymphoma, multiple liver lesions with no known history of cancer, hepatosplenomegaly or concurrent splenic lesions, vascular encasement without occlusion or thrombosis, and widespread adenopathy above and below the diaphragm. The possibility of a hematologic disorder may change management and obviate surgery. If biopsy is contemplated, core biopsy may be required instead of fine-needle aspiration to increase the possibility of correct diagnosis.

Figure 21. HLH in a 38-year-old man who presented with weight loss and flu-like illness. (a) US image shows multiple solid hypoechoic hepatic masses (arrow). (b) Axial CT image shows marked hepatosplenomegaly, with numerous hypoenhancing masses (arrow). (c) Coronal contrast-enhanced MR image shows numerous hypoenhancing lesions in the liver (arrowhead) and spleen (arrow), with hepatosplenomegaly. The findings are nonspecific, and the differential diagnosis includes metastases and lymphoma. Biopsy demonstrated HLH.



a.



b.



c.

Disclosures of Conflicts of Interest.—K.S. *Activities related to the present article:* disclosed no relevant relationships. *Activities not related to the present article:* grants from and consultant for Repligen Corp; grants from Siemens Medical Solutions and Philips Medical. *Other activities:* disclosed no relevant relationships.

References

- Izadi M, Fazel M, Saadat SH, Taheri S. Hepatic involvement by lymphoproliferative disorders post liver transplantation: PTLD. *Int. Survey. Hepatol Int* 2011;5(3):759–766.
- Leite NP, Kased N, Hanna RF, et al. Cross-sectional imaging of extranodal involvement in abdominopelvic lymphoproliferative malignancies. *RadioGraphics* 2007;27(6):1613–1634.
- Walz-Mattmüller R, Horny HP, Ruck P, Kaiserling E. Incidence and pattern of liver involvement in haematological malignancies. *Pathol Res Pract* 1998;194(11):781–789.
- Hu Q, Naushad H, Xie Q, Al-Howaidi I, Wang M, Fu K. Needle-core biopsy in the pathologic diagnosis of malignant lymphoma showing high reproducibility among pathologists. *Am J Clin Pathol* 2013;140(2):238–247.
- Elsayes KM, Menias CO, Willatt JM, Pandya A, Wiggins M, Platt J. Primary hepatic lymphoma: imaging findings. *J Med Imaging Radiat Oncol* 2009;53(4):373–379.
- Noronha V, Shafi NQ, Obando JA, Kummar S. Primary non-Hodgkin's lymphoma of the liver. *Crit Rev Oncol Hematol* 2005;53(3):199–207.
- Freeman C, Berg JW, Cutler SJ. Occurrence and prognosis of extranodal lymphomas. *Cancer* 1972;29(1):252–260.
- Caccamo D, Pervez NK, Marchevsky A. Primary lymphoma of the liver in the acquired immunodeficiency syndrome. *Arch Pathol Lab Med* 1986;110(6):553–555.
- Emile JF, Azoulay D, Gornet JM, et al. Primary non-Hodgkin's lymphomas of the liver with nodular and diffuse infiltration patterns have different prognoses. *Ann Oncol* 2001;12(7):1005–1010.
- Gazelle GS, Lee MJ, Hahn PF, Goldberg MA, Rafaat N, Mueller PR. US, CT, and MRI of primary and secondary liver lymphoma. *J Comput Assist Tomogr* 1994;18(3):412–415.
- Maher MM, McDermott SR, Fenlon HM, et al. Imaging of primary non-Hodgkin's lymphoma of the liver. *Clin Radiol* 2001;56(4):295–301.
- Sandrasegaran K, Robinson PJ, Selby P. Staging of lymphoma in adults. *Clin Radiol* 1994;49(3):149–161.
- Bach AG, Behrmann C, Holzhausen HJ, Spielmann RP, Surov A. Prevalence and imaging of hepatic involvement in malignant lymphoproliferative disease. *Clin Imaging* 2012;36(5):539–546.
- Foschi FG, Dall'Aglio AC, Marano G, et al. Role of contrast-enhanced ultrasonography in primary hepatic lymphoma. *J Ultrasound Med* 2010;29(9):1353–1356.
- Kwee TC, Takahara T, Vermoolen MA, Bierings MB, Mali WP, Nievelstein RA. Whole-body diffusion-weighted imaging for staging malignant lymphoma in children. *Pediatr Radiol* 2010;40(10):1592–1602; quiz 1720–1721.
- Lin C, Itti E, Luciani A, Haioun C, Meignan M, Rahmouni A. Whole-body diffusion-weighted imaging in lymphoma. *Cancer Imaging* 2010;10(Spec No A):S172–S178.
- van Ufford HM, Kwee TC, Beek FJ, et al. Newly diagnosed lymphoma: initial results with whole-body T1-weighted, STIR, and diffusion-weighted MRI compared with ¹⁸F-FDG PET/CT. *AJR Am J Roentgenol* 2011;196(3):662–669.
- Kaneko K, Nishie A, Arima F, et al. A case of diffuse-type primary hepatic lymphoma mimicking diffuse hepatocellular carcinoma. *Ann Nucl Med* 2011;25(4):303–307.
- Jerusalem G, Beguin Y, Najjar F, et al. Positron emission tomography (PET) with ¹⁸F-fluorodeoxyglucose (¹⁸F-FDG) for the staging of low-grade non-Hodgkin's lymphoma (NHL). *Ann Oncol* 2001;12(6):825–830.
- Bangerter M, Moog F, Griesshammer M, et al. Usefulness of FDG-PET in diagnosing primary lymphoma of the liver. *Int J Hematol* 1997;66(4):517–520.

21. Joshi PV, Lele VR, Bhat GM, Garg S, Chitale A. F-18 fluorodeoxyglucose positron emission tomography/computed tomography findings in a case of hepatosplenic T-cell lymphoma. *J Cancer Res Ther* 2012;8(1):106–108.
22. Pan B, Wang CS, Han JK, Zhan LF, Ni M, Xu SC. ¹⁸F-fluorodeoxyglucose PET/CT findings of a solitary primary hepatic lymphoma: a case report. *World J Gastroenterol* 2012;18(48):7409–7412.
23. Matsumoto S, Mori H, Takaki H, Ishitobi F, Shuto R, Yokoyama S. Malignant lymphoma with tumor thrombus in the portal venous system. *Abdom Imaging* 2004;29(4):460–462.
24. De Gaetano AM, Rufini V, Castaldi P, et al. Clinical applications of ¹⁸F-FDG PET in the management of hepatobiliary and pancreatic tumors. *Abdom Imaging* 2012;37(6):983–1003.
25. Levy M, Backman L, Husberg B, et al. De novo malignancy following liver transplantation: a single-center study. *Transplant Proc* 1993;25(1 Pt 2):1397–1399.
26. Green M, Webber S. Posttransplantation lymphoproliferative disorders. *Pediatr Clin North Am* 2003;50(6):1471–1491.
27. Harris NL, Swerdlow SH, Frizzera G, Knowles DM. Post-transplant lymphoproliferative disorders. In: Jaffe ES, Harris NL, Stein H, Vardiman JW, eds. *World Health Organization classification of tumours: pathology and genetics of tumours of haematopoietic and lymphoid tissues*. Lyon, France: IARC, 2001; 264–269.
28. Jagadeesh D, Woda BA, Draper J, Evens AM. Post transplant lymphoproliferative disorders: risk, classification, and therapeutic recommendations. *Curr Treat Options Oncol* 2012;13(1):122–136.
29. Glotz D, Chapman JR, Dharnidharka VR, et al. The Seville expert workshop for progress in posttransplant lymphoproliferative disorders. *Transplantation* 2012;94(8):784–793.
30. Bakker NA, van Imhoff GW, Verschuuren EA, van Son WJ. Presentation and early detection of post-transplant lymphoproliferative disorder after solid organ transplantation. *Transpl Int* 2007;20(3):207–218.
31. Jeon TY, Kim JH, Eo H, et al. Posttransplantation lymphoproliferative disorder in children: manifestations in hematopoietic cell recipients in comparison with liver recipients. *Radiology* 2010;257(2):490–497.
32. LaCasce AS. Post-transplant lymphoproliferative disorders. *Oncologist* 2006;11(6):674–680.
33. Pickhardt PJ, Siegel MJ. Posttransplantation lymphoproliferative disorder of the abdomen: CT evaluation in 51 patients. *Radiology* 1999;213(1):73–78.
34. Borhani AA, Hosseinzadeh K, Almusa O, Furlan A, Nalesnik M. Imaging of posttransplantation lymphoproliferative disorder after solid organ transplantation. *RadioGraphics* 2009;29(4):981–1000; discussion 1000–1002.
35. Dhillon MS, Rai JK, Gunson BK, Olliff S, Olliff J. Post-transplant lymphoproliferative disease in liver transplantation. *Br J Radiol* 2007;80(953):337–346.
36. Scarsbrook AF, Warakalle DR, Dattani M, Traill Z. Post-transplantation lymphoproliferative disorder: the spectrum of imaging appearances. *Clin Radiol* 2005;60(1):47–55.
37. Blaes AH, Cioc AM, Froelich JW, Peterson BA, Dunitz JM. Positron emission tomography scanning in the setting of post-transplant lymphoproliferative disorders. *Clin Transplant* 2009;23(6):794–799.
38. Chowdhury FU, Sheerin F, Bradley KM, Gleeson FV. PET/CT staging and response evaluation of post-transplantation lymphoproliferative disease (PTLD). *Clin Nucl Med* 2009;34(6):386–387.
39. Regalia E, Fassati LR, Valente U, et al. Pattern and management of recurrent hepatocellular carcinoma after liver transplantation. *J Hepatobiliary Pancreat Surg* 1998;5(1):29–34.
40. Schlitt HJ, Neipp M, Weimann A, et al. Recurrence patterns of hepatocellular and fibrolamellar carcinoma after liver transplantation. *J Clin Oncol* 1999;17(1):324–331.
41. Lee EY, Anthony MP, Leung AY, Loong F, Khong PL. Utility of FDG PET/CT in the assessment of myeloid sarcoma. *AJR Am J Roentgenol* 2012;198(5):1175–1179.
42. Mantzarides M, Bonardel G, Fagot T, et al. Granulocytic sarcomas evaluated with F-18-fluorodeoxyglucose PET. *Clin Nucl Med* 2008;33(2):115–117.
43. Neiman RS, Barcos M, Berard C, et al. Granulocytic sarcoma: a clinicopathologic study of 61 biopsied cases. *Cancer* 1981;48(6):1426–1437.
44. Shinagare AB, Krajewski KM, Hornick JL, et al. MRI for evaluation of myeloid sarcoma in adults: a single-institution 10-year experience. *AJR Am J Roentgenol* 2012;199(6):1193–1198.
45. Klcio JM, Welch JS, Nguyen TT, et al. State of the art in myeloid sarcoma. *Int J Lab Hematol* 2011;33(6):555–565.
46. Wandroo FA, Murray J, Mutimer D, Hubscher S. Acute myeloid leukaemia presenting as cholestatic hepatitis. *J Clin Pathol* 2004;57(5):544–545.
47. Bakst R, Wolden S, Yahalom J. Radiation therapy for chloroma (granulocytic sarcoma). *Int J Radiat Oncol Biol Phys* 2012;82(5):1816–1822.
48. Yilmaz AF, Saydam G, Sahin F, Baran Y. Granulocytic sarcoma: a systematic review. *Am J Blood Res* 2013;3(4):265–270.
49. Mahgerefteh SY, Sosna J, Bogot N, Shapira MY, Pappo O, Bloom AI. Radiologic imaging and intervention for gastrointestinal and hepatic complications of hematopoietic stem cell transplantation. *Radiology* 2011;258(3):660–671.
50. Hartleb M, Gutkowski K, Milkiewicz P. Nodular regenerative hyperplasia: evolving concepts on underdiagnosed cause of portal hypertension. *World J Gastroenterol* 2011;17(11):1400–1409.
51. Levine DS, Navarro OM, Chaudry G, Doyle JJ, Blaser SI. Imaging the complications of bone marrow transplantation in children. *RadioGraphics* 2007;27(2):307–324.
52. Hall MN, Jagannathan JP, Ramaiya NH, Shinagare AB, Van den Abbeele AD. Imaging of extraosseous myeloma: CT, PET/CT, and MRI features. *AJR Am J Roentgenol* 2010;195(5):1057–1065.
53. Philips S, Menias C, Vikram R, Sunnapwar A, Prasad SR. Abdominal manifestations of extraosseous myeloma: cross-sectional imaging spectrum. *J Comput Assist Tomogr* 2012;36(2):207–212.
54. Oshima K, Kanda Y, Nannya Y, et al. Clinical and pathologic findings in 52 consecutively autopsied cases with multiple myeloma. *Am J Hematol* 2001;67(1):1–5.
55. Varettoni M, Corso A, Pica G, Mangiacavalli S, Pascutto C, Lazzarino M. Incidence, presenting features and outcome of extramedullary disease in multiple myeloma: a longitudinal study on 1003 consecutive patients. *Ann Oncol* 2010;21(2):325–330.
56. Thomas FB, Clausen KP, Greenberger NJ. Liver disease in multiple myeloma. *Arch Intern Med* 1973;132(2):195–202.
57. Mouloupoulos LA, Granfield CA, Dimopoulos MA, Kim EE, Alexanian R, Libshitz HI. Extraosseous multiple myeloma: imaging features. *AJR Am J Roentgenol* 1993;161(5):1083–1087.
58. Simmons MZ, Miller JA, Levine CD, Glucksman WJ, Wachsberg RH. Myelomatous involvement of the liver: unusual ultrasound appearance. *J Clin Ultrasound* 1997;25(3):145–148.
59. Birjawi GA, Jalbout R, Musallam KM, Tawil AN, Taher AT, Khoury NJ. Abdominal manifestations of multiple myeloma: a retrospective radiologic overview. *Clin Lymphoma Myeloma* 2008;8(6):348–351.
60. Kelekis NL, Semelka RC, Warshauer DM, Sallah S. Nodular liver involvement in light chain multiple myeloma: appearance on US and MRI. *Clin Imaging* 1997;21(3):207–209.
61. Cerrato C, Palumbo A. Initial treatment of nontransplant patients with multiple myeloma. *Semin Oncol* 2013;40(5):577–584.
62. Fonseca R, Monge J. Myeloma: classification and risk assessment. *Semin Oncol* 2013;40(5):554–566.
63. Girnius S, Munshi NC. Individualized therapy in multiple myeloma: are we there? *Semin Oncol* 2013;40(5):567–576.
64. Moreau P, Touzeau C. Initial treatment of transplant candidates with multiple myeloma. *Semin Oncol* 2013;40(5):585–591.
65. Bonekamp D, Horton KM, Hruban RH, Fishman EK. Castleman disease: the great mimic. *RadioGraphics* 2011;31(6):1793–1807.

66. Herrada J, Cabanillas F, Rice L, Manning J, Pugh W. The clinical behavior of localized and multicentric Castleman disease. *Ann Intern Med* 1998;128(8):657-662.
67. Rahmouni A, Golli M, Mathieu D, Anglade MC, Charlotte F, Vasile N. Castleman disease mimicking liver tumor: CT and MR features. *J Comput Assist Tomogr* 1992;16(5):699-703.
68. Cronin DM, Warnke RA. Castleman disease: an update on classification and the spectrum of associated lesions. *Adv Anat Pathol* 2009;16(4):236-246.
69. McAdams HP, Rosado-de-Christenson M, Fishback NF, Templeton PA. Castleman disease of the thorax: radiologic features with clinical and histopathologic correlation. *Radiology* 1998;209(1):221-228.
70. Carucci LR, Halvorsen RA. Abdominal and pelvic CT in the HIV-positive population. *Abdom Imaging* 2004;29(6):631-642.
71. Uldrick TS, Polizzotto MN, Yarchoan R. Recent advances in Kaposi sarcoma herpes virus-associated multicentric Castleman disease. *Curr Opin Oncol* 2012;24(5):495-505.
72. Reddy D, Mitsuyasu R. HIV-associated multicentric Castleman disease. *Curr Opin Oncol* 2011;23(5):475-481.
73. Saeed-Abdul-Rahman I, Al-Amri AM. Castleman disease. *Korean J Hepatol* 2012;47(3):163-177.
74. Bandera B, Ainsworth C, Shikle J, Rupard E, Roach M. Treatment of unicentric Castleman disease with neoadjuvant rituximab. *Chest* 2010;138(5):1239-1241.
75. Deiva K, Mahlaoui N, Beaudonnet F, et al. CNS involvement at the onset of primary hemophagocytic lymphohistiocytosis. *Neurology* 2012;78(15):1150-1156.
76. Henter JL, Elinder G, Ost A. Diagnostic guidelines for hemophagocytic lymphohistiocytosis: the FHL Study Group of the Histiocyte Society. *Semin Oncol* 1991;18(1):29-33.
77. Kim MM, Yum MS, Choi HW, et al. Central nervous system (CNS) involvement is a critical prognostic factor for hemophagocytic lymphohistiocytosis. *Korean J Hepatol* 2012;47(4):273-280.
78. Ozgen B, Karli-Oguz K, Sarikaya B, Tavil B, Gurgey A. Diffusion-weighted cranial MR imaging findings in a patient with hemophagocytic syndrome. *AJNR Am J Neuroradiol* 2006;27(6):1312-1314.
79. Ruppert P, Edmonds EC, Brook M, Musil S, Han SD. Neuropsychological assessment in a case of adult-onset hemophagocytic lymphohistiocytosis (HLH). *Clin Neuropsychol* 2012;26(6):1038-1052.